

Dimorphism of 1,4-dibromo-2,5-bis(bromomethyl)benzene: Crystallographic and physico-chemical investigations

Christian Näther, Inke Jess, Piotr Kuś and Peter G. Jones

Supplementary Material

Fig. S1	XRPD patterns for two different batches of the material obtained from the synthesis and XRPD patterns for form I and form II calculated from single crystal data measured at room-temperature.	2
Fig. S2	Microscopic images of form I and form II and of batch 1, which consists of a mixture of both forms with form I as the major phase.	3
Fig. S3	DSC heating and cooling cycles at 10°C/min for batch 1, which consists of a mixture of form I and II with form I as the major phase.	3
Fig. S4	Experimental XRPD pattern of the residue obtained after the first small endothermic event observed in the DSC measurement of batch 1 together with the pattern calculated for form I (bottom).	4
Fig. S5	DSC curves for batch 2, which consists of form I , at various heating rates.	4
Tab. S1	Peak and onset temperatures and heat of fusion ΔH_{fus} measured at various heating rates for batch 2, which according to XRPD consists of form I exclusively.	5
Fig. S6	DSC heating and cooling cycles for batch 2, which consists of form I , measured at 10 °C.	5
Fig. S7	Experimental XRPD pattern of the residue isolated at 120 °C in one DSC run measured for batch 2, together with the pattern calculated for form II .	6
Fig. S8	Experimental XRPD pattern as function of temperature for batch 2, which consists of form I .	6
Fig. S9	Experimental XRPD pattern for the solidified melt of batch 1 together with the pattern calculated for form I .	7
Fig. S10	Heating-rate-dependent DSC curves for form I , obtained by consecutive heating and cooling cycles of the melt obtained from batch 1.	7
Tab. S2	Peak and onset temperatures and heat of fusion for pure form I (obtained by melting of batch 1) measured at different heating rates.	8
Fig. S11	Experimental XRPD pattern of two different residues, each obtained by fast evaporation of the solvent from a solution of the material in dichloromethane, together with the calculated pattern for form I and II .	9
Fig. S12	Experimental XRPD pattern of a mixture of form I and II and of the residues after stirring this mixture in different solvents for one week, together with the calculated pattern for form I and form II .	9
Fig. S13	Experimental XRPD pattern as function of temperature for a mixture of form I and form II .	10
Fig. S14	Experimental XRPD pattern as function of temperature for pure form II .	10
Fig. S15	DSC curves for form II at various heating rates.	10
Tab. S3	Peak and onset temperatures and heat of fusion for form II measured at various heating rates.	11
Fig. S16	DSC curves of batch 1 at 0.1°C/min.	11

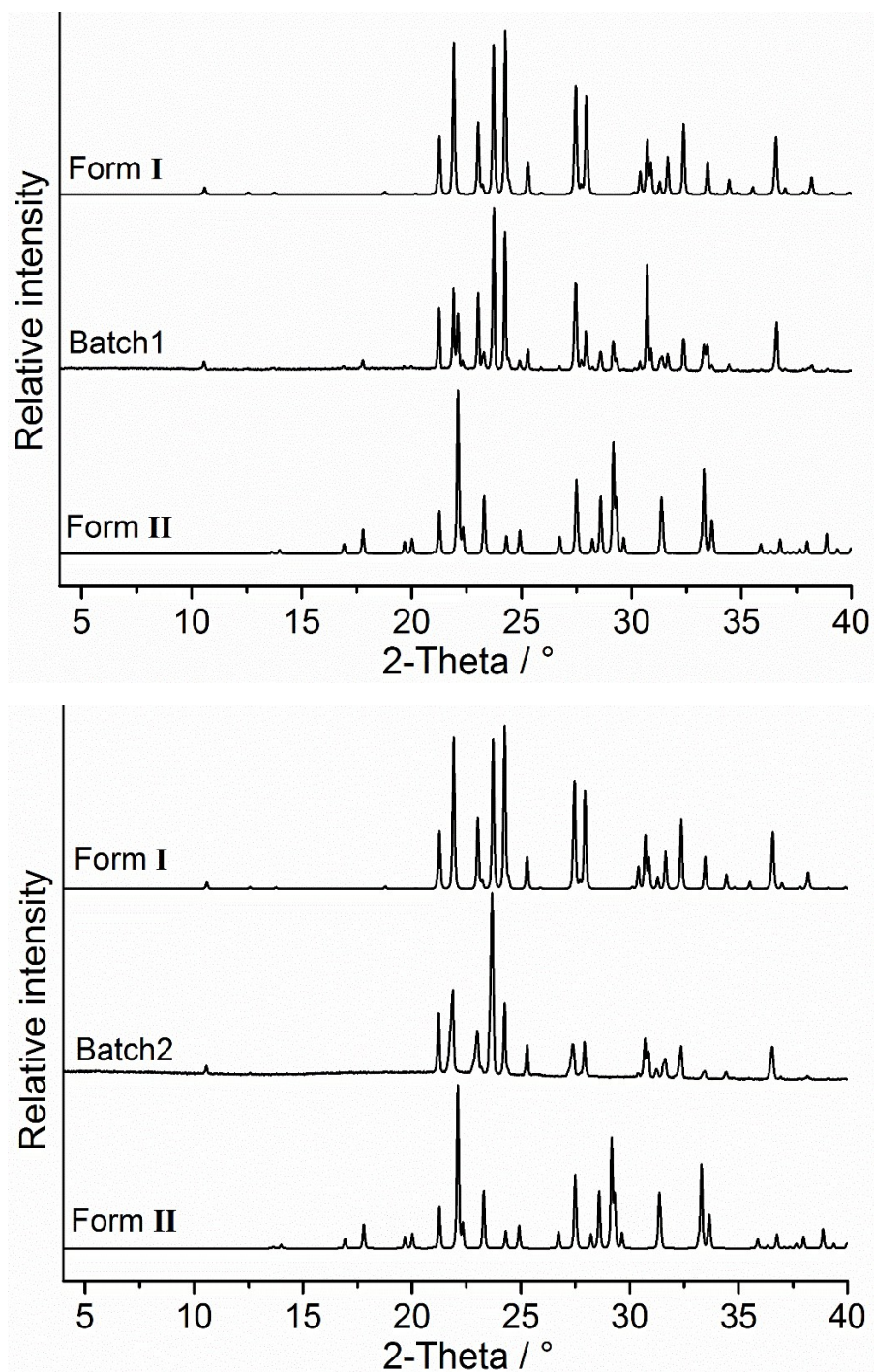


Fig. S1. XRPD patterns for two different batches (1 and 2) of the material obtained from the synthesis and XRPD patterns for form I and form II calculated from single crystal data measured at room-temperature. Batch 1 consists of a mixture of both forms with form I as the major phase.

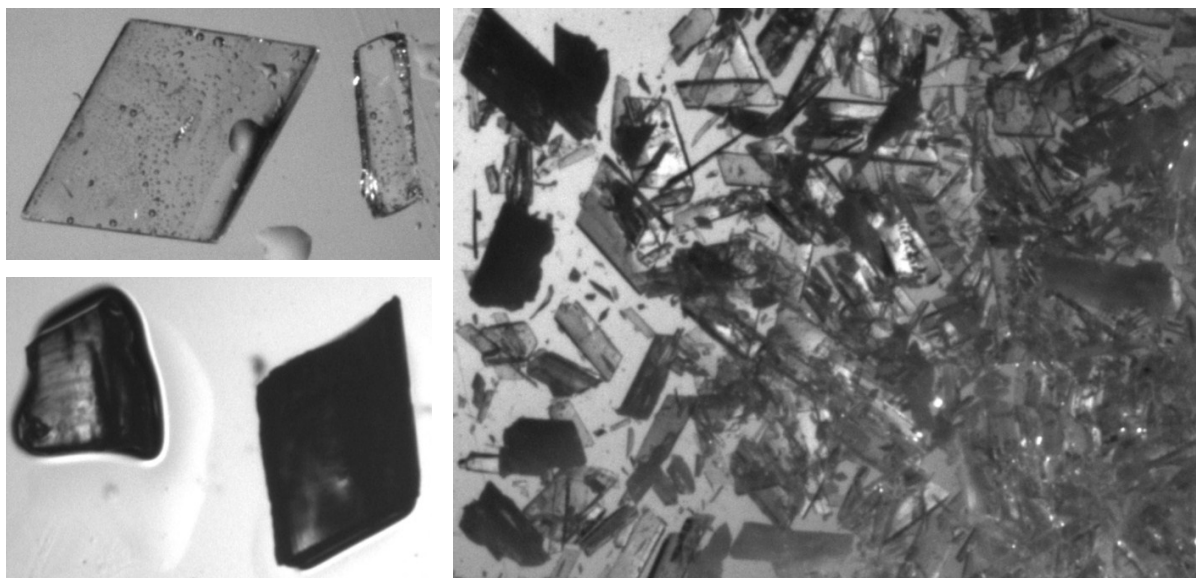


Fig. S2. Microscopic images of form I (left, top) and form II (left, bottom) and of batch 1, which consists of a mixture of both forms with form I (the brighter crystals) as the major phase (right).

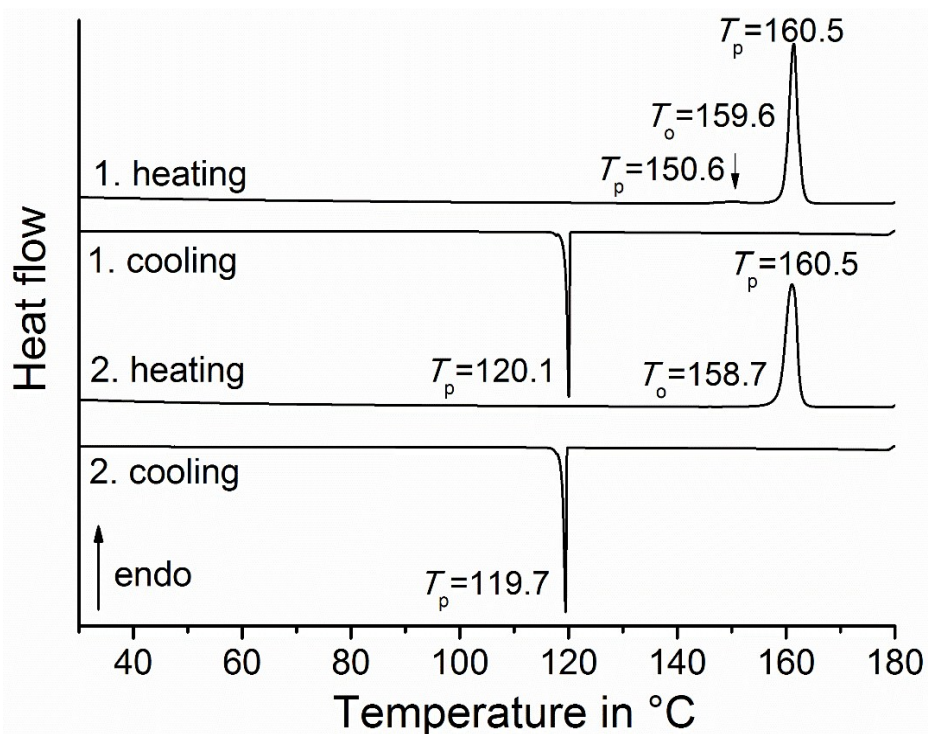


Fig. S3. DSC heating and cooling cycles at 10°C/min for batch 1, which consists of a mixture of form I and II with form I as the major phase. The peak (T_p) and onset (T_o) temperatures are given in °C.

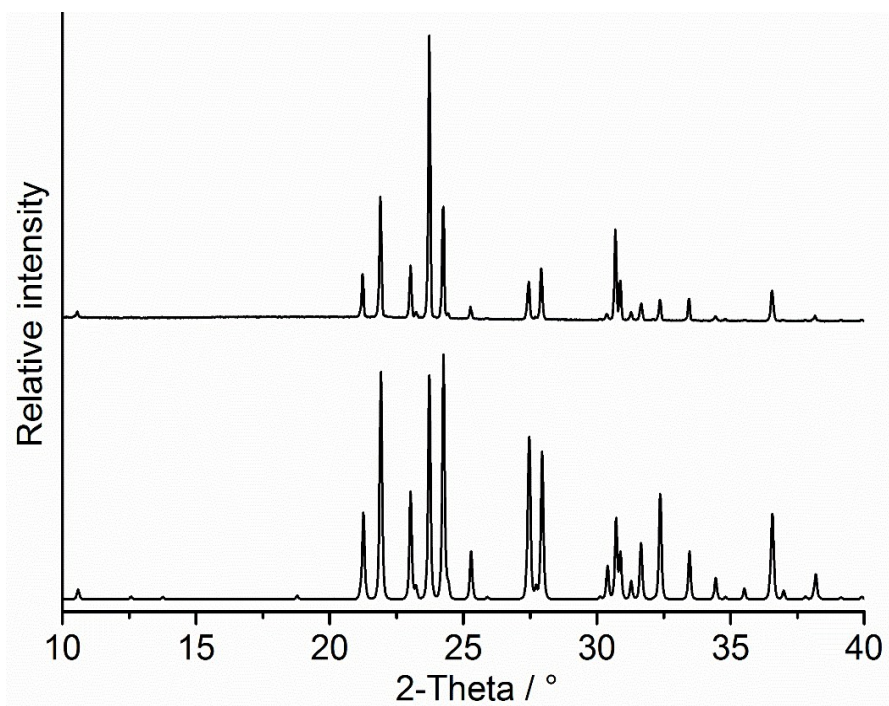


Fig. S4. Experimental XRPD pattern of the residue obtained after the first small endothermic event observed in the DSC measurement of batch 1, together with the pattern calculated for form I (bottom).

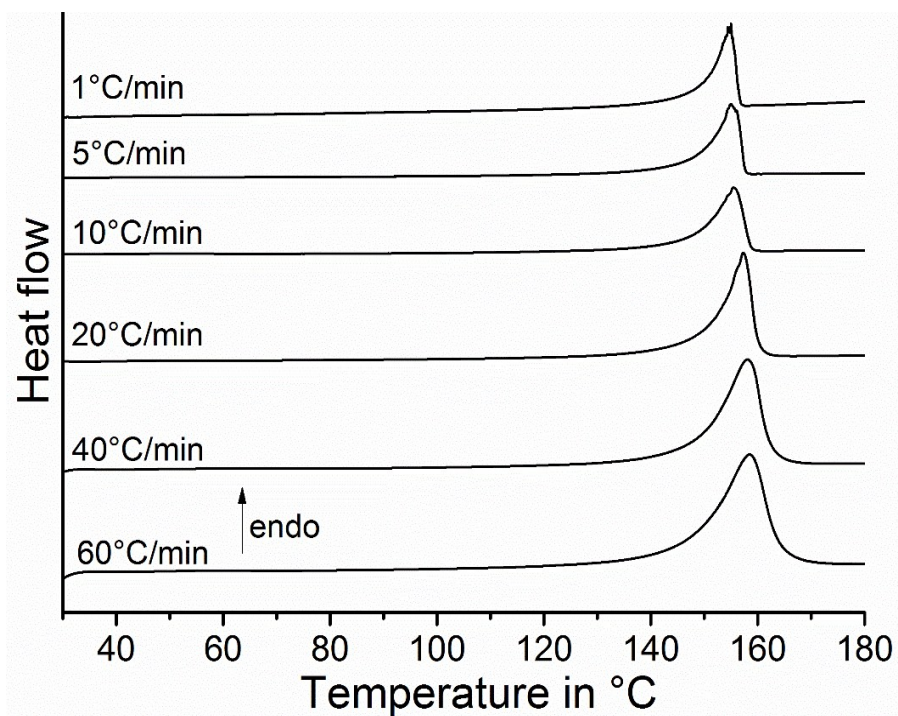


Fig. S5. DSC curves for batch 2, which consists of form I, at different heating rates.

Table S1. Peak (T_p) and onset (T_o) temperatures and heat of fusion ΔH_{fus} measured at various heating rates for batch 2, which according to XRPD consists of form I exclusively.

Heating rate in °C/min	T_p in °C	T_o in °C	ΔH_{fus} in kJ/mol
1	154.9	149.4	24.5
5	154.9	152.1	27.4
10	155.1	151.3	28.9
20	156.6	152.2	28.1
40	157.0	148.6	26.8
60	157.3	147.2	26.8

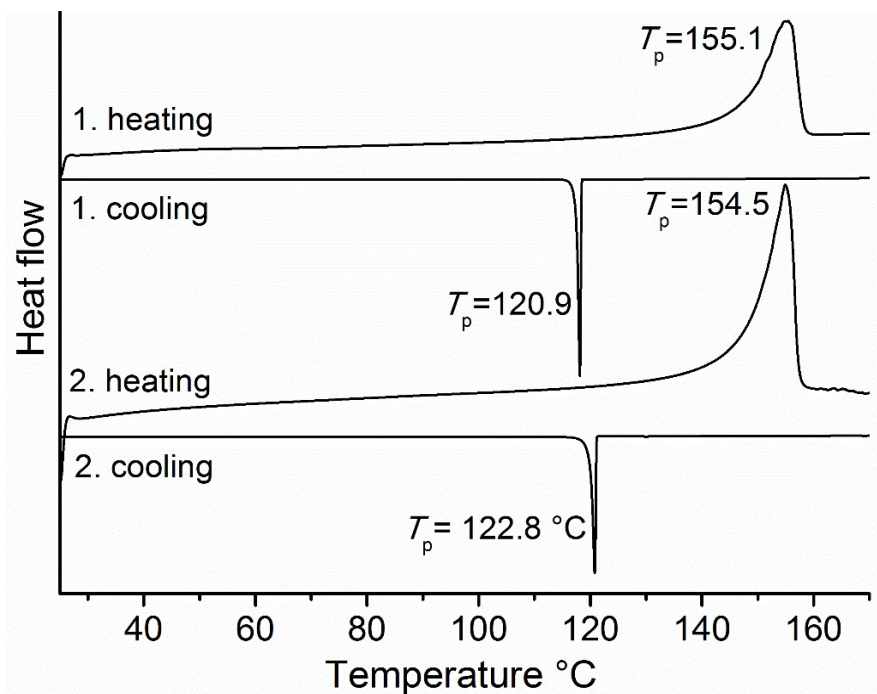


Fig. S6. DSC heating and cooling cycles for batch 2, which consists of form I, measured at 10 °C. The peak (T_p) and onset (T_o) temperatures are given in °C.

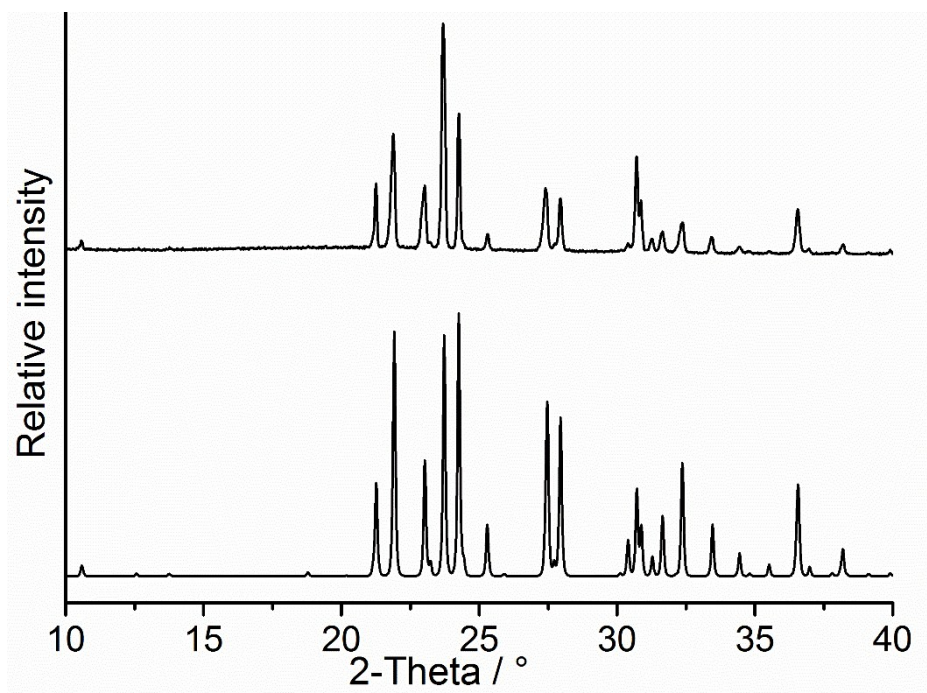


Fig. S7. Experimental (top) XRPD pattern of the residue isolated at 120 °C in one DSC run measured for batch 2, together with the pattern calculated for form I (bottom).

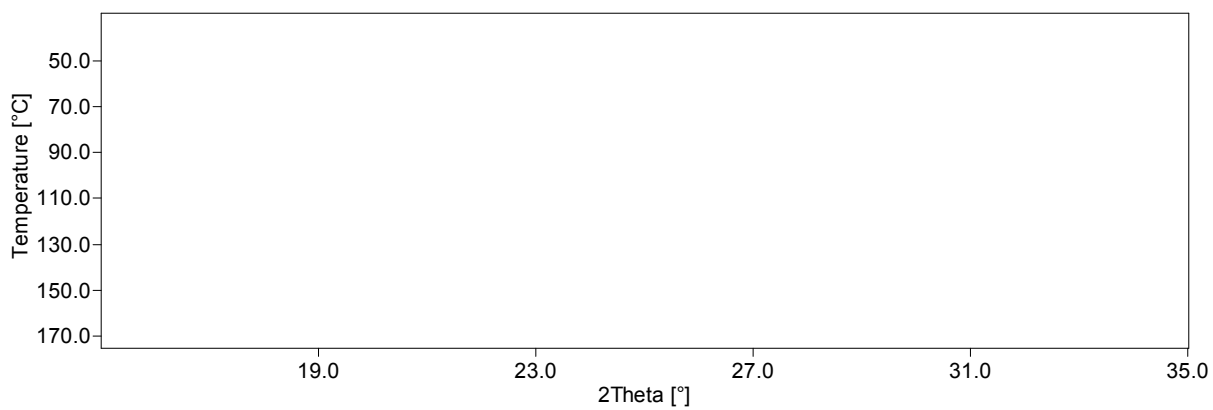


Figure S8: Experimental XRPD pattern as function of temperature for batch 2, which consists of form I.

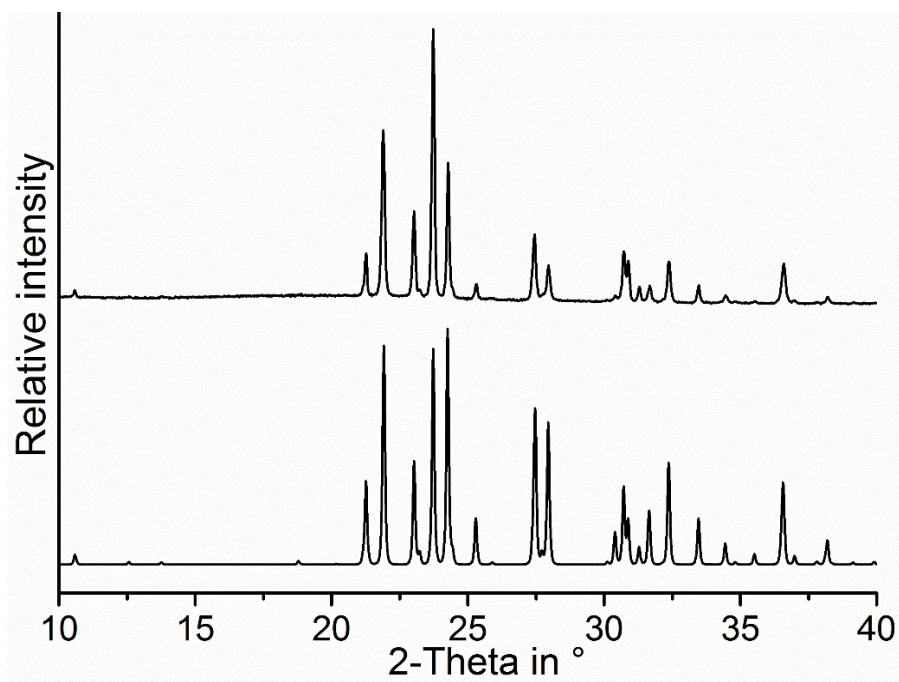


Fig. S9. Experimental (top) XRPD pattern of the solidified melt of batch 1, together with the pattern calculated for form I (bottom).

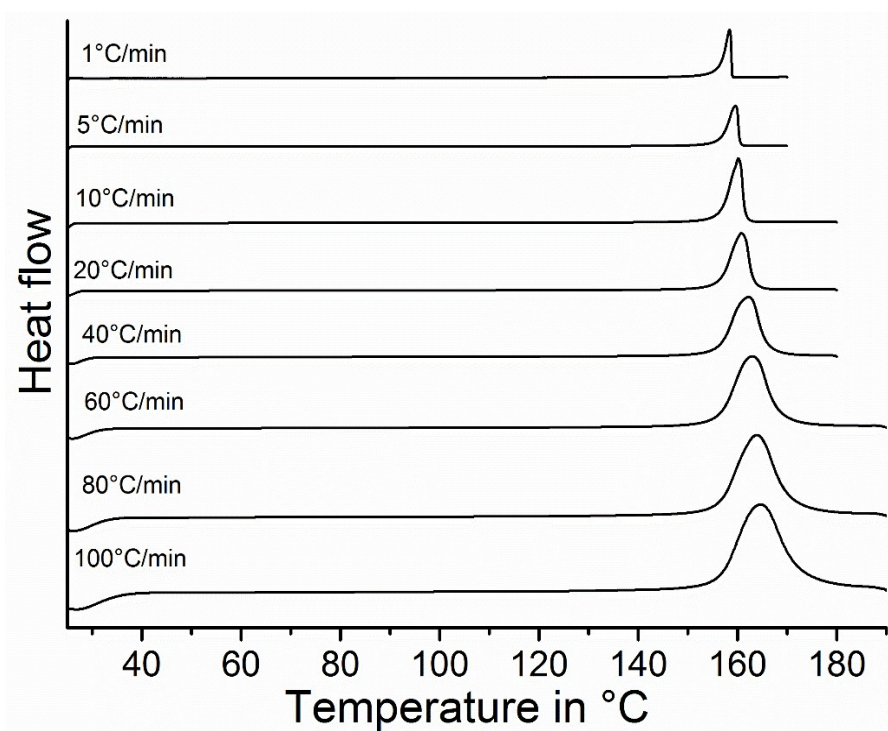


Fig. S10. Heating-rate-dependent DSC curves for form I, obtained by consecutive heating and cooling cycles of the melt obtained from batch 1.

Table S2. Peak (T_p) and onset (T_o) temperatures and heat of fusion ΔH_{fus} for pure form I (obtained by melting of batch 1) measured at various heating rates.

	Heating rate/ °C/min	ΔH /kJ/mol	Onset temp. / °C	Peak temp. / °C
1st heating	1	27.9	156.4	158.2
2nd heating	1	28.4	156.8	158.4
3rd heating	1	27.9	157.0	158.5
4th heating	1	28.1	157.1	158.6
5th heating	1	27.6	157.2	158.7
Average		28.0	156.9	158.5
<hr/>				
1st heating	5	27.5	156.5	159.1
2nd heating	5	27.2	156.7	159.0
3rd heating	5	27.0	156.8	159.0
4th heating	5	26.8	156.6	159.1
5th heating	5	26.6	156.8	159.2
Average		27.0	156.7	159.1
<hr/>				
1st heating	10	26.7	156.3	159.3
2nd heating	10	26.3	156.3	159.4
3rd heating	10	26.1	156.4	159.5
4th heating	10	25.9	156.5	159.3
5th heating	10	25.7	156.4	159.3
Average		26.2	156.4	159.4
<hr/>				
1st heating	20	25.7	156.1	159.6
2nd heating	20	25.4	156.0	159.6
3rd heating	20	25.4	156.1	159.9
4th heating	20	25.2	156.1	159.9
5th heating	20	25.2	156.1	159.9
Average		25.4	156.1	159.8
<hr/>				
1st heating	40	25.0	155.8	160.5
2nd heating	40	24.8	155.7	160.0
3rd heating	40	24.8	155.7	160.3
4th heating	40	24.5	155.7	160.4
5th heating	40	24.7	155.7	160.5
Average		24.8	155.7	160.3
<hr/>				
1st heating	60	25.0	155.5	160.9
2nd heating	60	24.8	155.9	161.1
3rd heating	60	24.7	155.8	160.9
4th heating	60	24.5	155.8	160.0
5th heating	60	24.6	155.7	161.0
Average		24.8	155.7	160.8

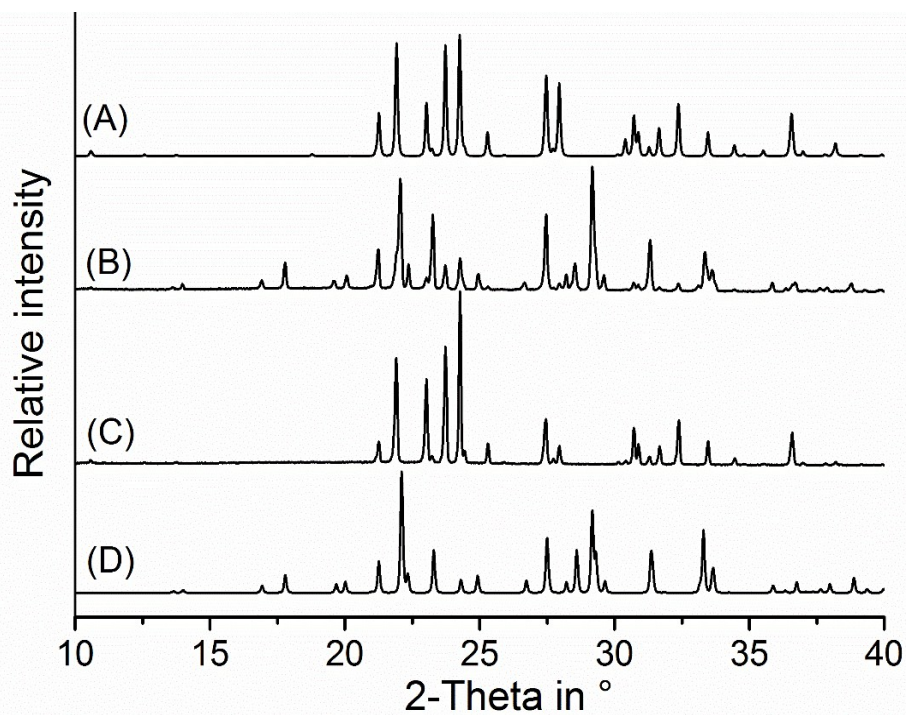


Fig. S11. Experimental XRPD pattern of two different residues, each obtained by fast evaporation of the solvent from a solution of the material in dichloromethane (B and C) together with the calculated pattern for form I (A) and II (D).

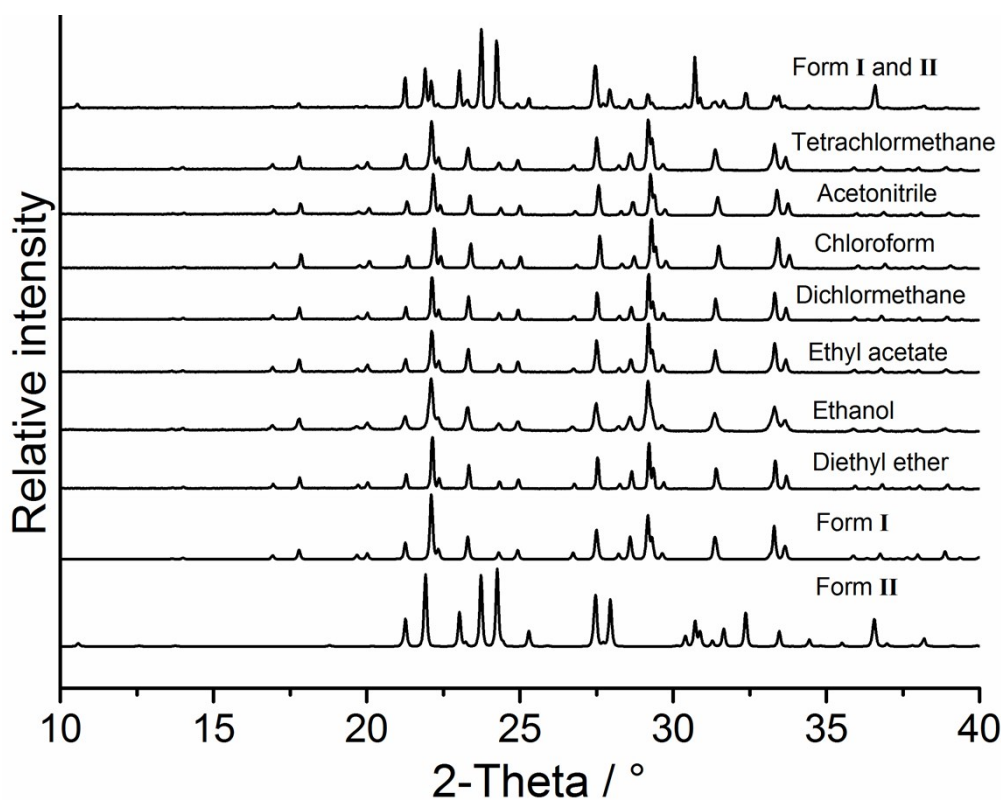


Figure S12: Experimental XRPD pattern of a mixture of form I and II and of the residues after stirring this mixture in different solvents for one week together with the calculated pattern for form I and form II.

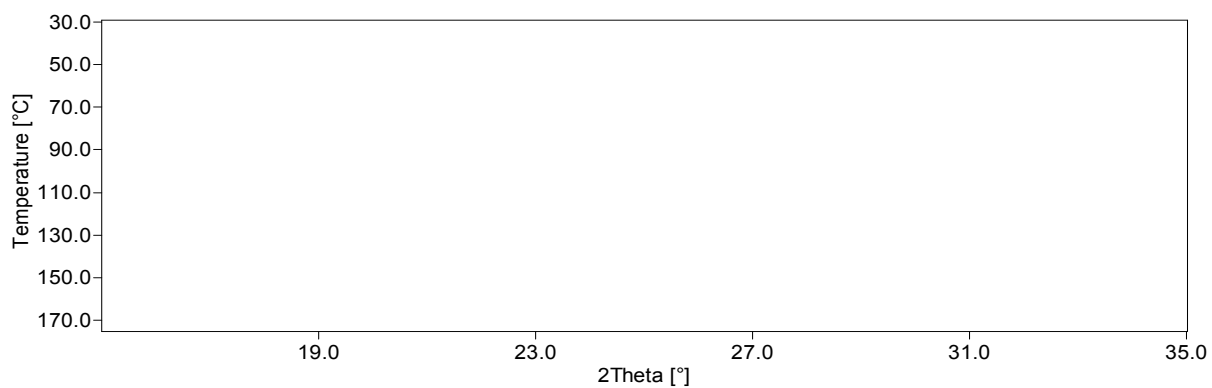


Figure S13: Experimental XRPD pattern as a function of temperature for a mixture of form **I** and form **II**.

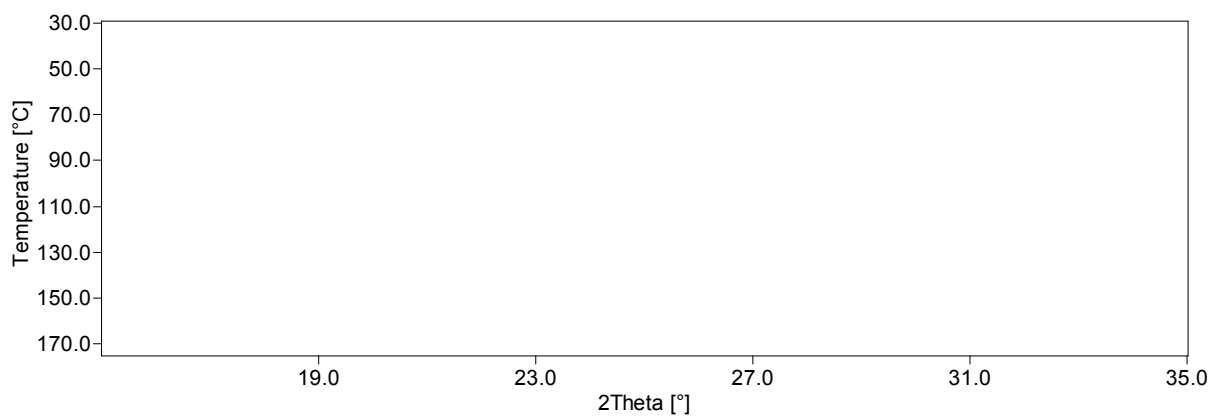


Figure S14: Experimental XRPD pattern as a function of temperature for pure form **II**.

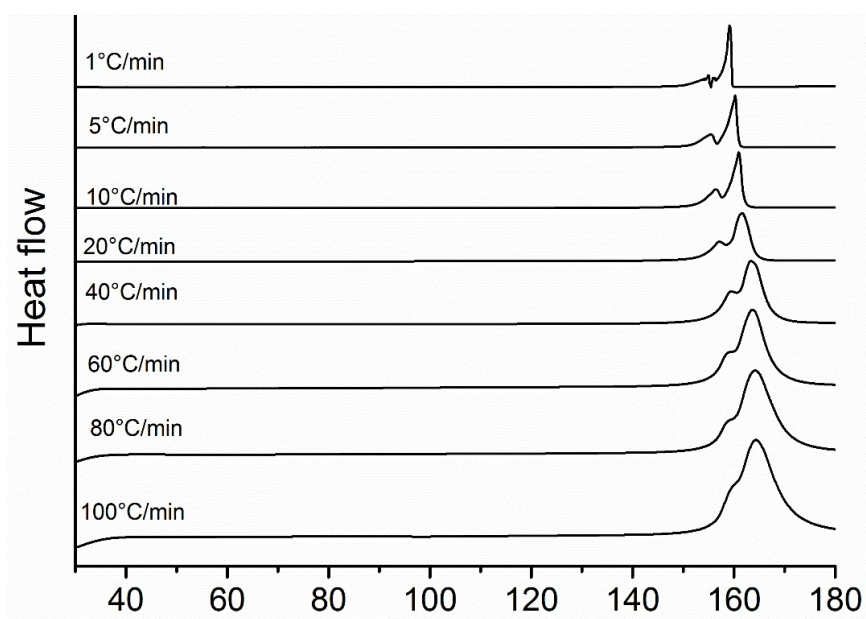


Figure S15: DSC curves for form **II** at various heating rates.

Table S3. Peak (T_p) and onset (T_o) temperatures and heat of fusion ΔH_{fus} for form II measured at various heating rates. 1 and 2 correspond to the sequence of the thermal events.

$^{\circ}\text{C}/\text{min}$	T_p in $^{\circ}\text{C}/1$	T_p in $^{\circ}\text{C}/2$	T_o in $^{\circ}\text{C}_1$	T_o in $^{\circ}\text{C}_2$	ΔH_{fus} in kJ/mol
1	155.1	158.9	149.2	157.4	32.7
5	155.3	159.7	151.1	157.4	31.5
10	156.4	160.1	153.1	157.1	33.9
20	157.2	160.4	153.2	157.8	33.5
40	159.7	161.5	153.7	158.8	33.8
Average	156.7	160.1	152.1	157.7	33.1

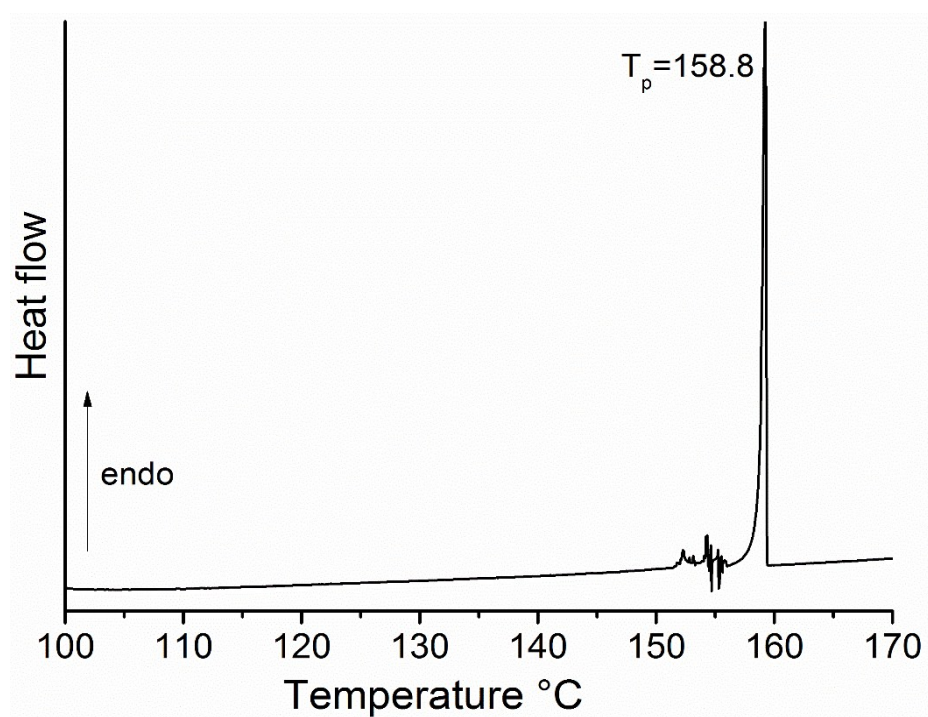


Figure S16: DSC curves of batch 1 at $0.1^{\circ}\text{C}/\text{min}$.